

AirMISR spectral and radiometric performance studies

Carol J. Bruegge, Wedad A. Abdou, Nadine L. Chrien, Barbara J. Gaitley

Jet Propulsion Laboratory, California Institute of Technology

4800 Oak Grove Dr., Pasadena, Ca. 91109

ABSTRACT

An Airborne Multi-angle Imaging SpectroRadiometer (AirMISR) instrument has been developed to assist in validation of the Earth Observing System (EOS) MISR experiment. The airborne instrument is built to the same performance specifications as MISR. Both instruments view the earth at nine discrete view angles, provide data products which are radiance scaled to Système International (SI) units, registered among the view angles, and geolocated. Whereas on-orbit MISR will acquire a global data set every nine days, the aircraft version is restricted to a target size of 9 x 11 km per aircraft run. AirMISR does, however, have the advantages of offering a means to testbed new mission procedures or camera designs, provide data sets which predate the MISR launch, and a means of returning to the laboratory to update the camera calibrations. This paper provides the AirMISR laboratory calibration results, as well as an example of a vicarious calibration exercise.

1. INTRODUCTION

The Multi-angle Imaging SpectroRadiometer (MISR)¹ instrument will launch aboard the first Earth Observing System spacecraft (EOS-AM1). MISR uses nine separate charge coupled device (CCD)-based pushbroom cameras to observe the earth at nine discrete angles; one at nadir plus eight other symmetrically placed cameras that provide fore-aft observations with view angles, at the earth's surface, of 26.1, 45.6, 60.0, and 70.0° relative to the local vertical. Each camera contains four detector line arrays, each overlain by a spectral filter providing imagery at four spectral bands within the visible and near-infrared (NIR).

The purpose of flying an additional instrument, AirMISR, is to collect MISR-like data sets to support in the development and validation of MISR data products, and to provide a verification of the EOS-AM1 MISR sensor calibration. It is believed, however, that AirMISR data will enable scientific research irrespective of MISR, in that program objectives are to produce high-quality, well calibrated multi-angle imaging data sets.

The AirMISR instrument flies on an ER-2 aircraft, and collects data at an altitude of 20 km. Unlike the EOS MISR, which contains nine individual cameras pointed at discrete look angles, AirMISR utilizes a single camera in a pivoting gimbal mount. A schematic of the flight view-angle sequence is shown in Figure 1. The camera has been fabricated from MISR brassboard and engineering model components², and thus has similar radiometric and spectral response as the MISR cameras. Another difference between the MISR and AirMISR cameras is in the focal plane temperature. The MISR focal plane is temperature-stabilized at -5° C; whereas the AirMISR focal plane temperature is controlled by the Optical Mechanical Structure temperature controller, ~ 25° C. The added dark current for the AirMISR camera is not sufficient to affect science performance.

2. SPECTRAL CALIBRATION

During MISR spectral calibration, the response profile was measured at three field positions and for nine cameras, for each of the four spectral bands. These data were found to be similar enough, and an averaged profile was adopted. These "Standardized spectral response profiles" are reported within the Ancillary Radiometric Product (ARP), a data file used in MISR standard product production. Data are from 365 to 1100 nm, in 0.5 nm steps, with a spectral resolution of 2.6 nm for the in-band region, and 19.6 nm otherwise. The spectral parameters quoted for MISR result from a solar-weighted, in-band moments analysis of the Standardized spectral response profiles. These parameters are 446.3, 557.5, 671.8, and 866.5 nm for center wavelength, and 40.9, 27.2, 20.4, and 38.6 nm for bandwidth.

The same laboratory facilities and procedures³ used for MISR calibration have been used for AirMISR calibration. Though measured spectral response data are available, AirMISR data product generation will make use of the MISR standardized

parameters. It is believe the simplification to processing outweighs any slight advantage to be gained in using the original measurements. A comparison between the standardized values and those measured specifically on the AirMISR camera are given in Table 1. The MISR out-of-band responses are listed for the range of values found within the nine cameras. AirMISR Band 3/ Red is shown to have an out-of-band response twice that of any MISR camera. It is noted that this focal plane was deliberately bypassed during the MISR build, in that better performance was found on alternate units. The measured AirMISR spectral scans are shown in Figures 2-5, and highlights the out-of-band leak in the Red Band. The dashed line at the 0.001 level of transmittance represents the MISR specification on peak out-of-band transmittance. The dashed line at 0.0001 represents the specification on out-of-band, averaged over 100 nm intervals.

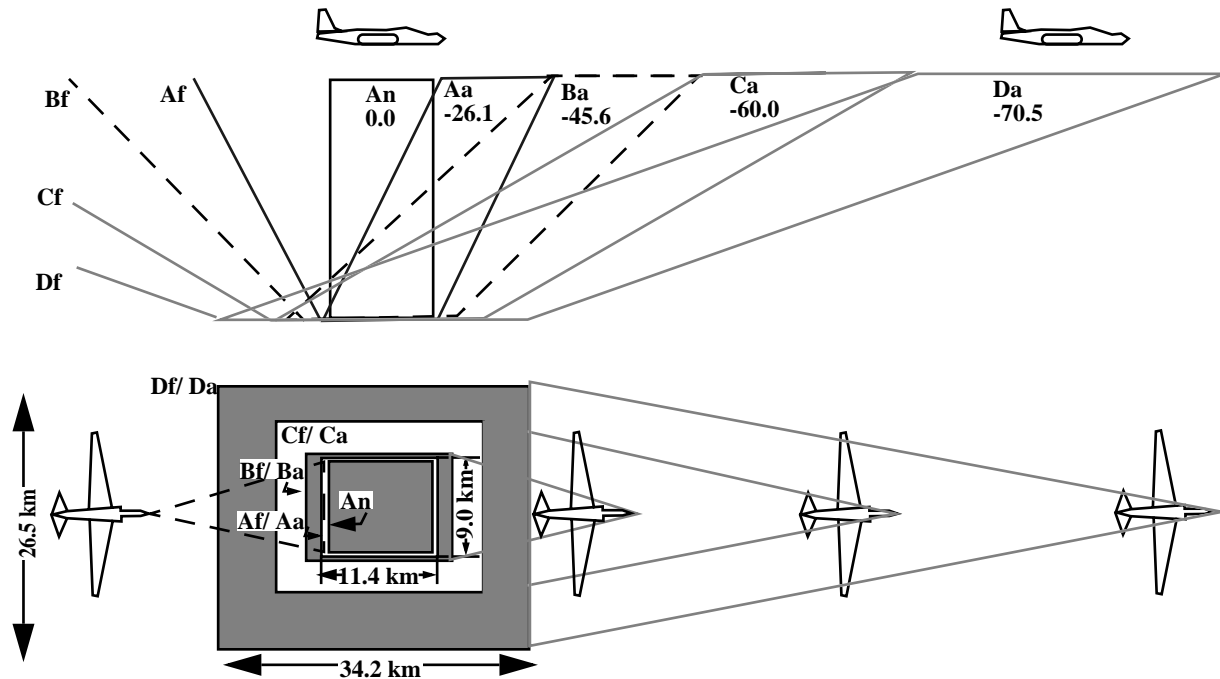


Figure 1. AirMISR gimbaling scheme used to acquire data at nine view angles.

Table 1. A comparison of MISR/ AirMISR spectral parameters

Parameter	MISR standardized values				AirMISR measured values			
	Band 1	Band 2	Band 3	Band 4	Band 1	Band 2	Band 3	Band 4
In-band, best fit gaussian center wavelength, nm	442.5	557.3	671.7	864.9	443.1	558.4	671.8	865.2
In-band, best-fit gaussian FWHM, nm	26.8	18.0	14.9	27.3	31.4	18.7	15.2	29.0
Total-band, moments analysis center wavelength, nm	446.9	558.6	670.1	861.2	448.1	560.7	668.3	863.5
Total-band, moments analysis spectral bandwidth, nm	79.0	90.1	92.8	147.1	93.4	95.0	132.3	109.6
Out-of-band response, %	1	2-3	2	0.8-2	0.87	2.32	4.92	1.80

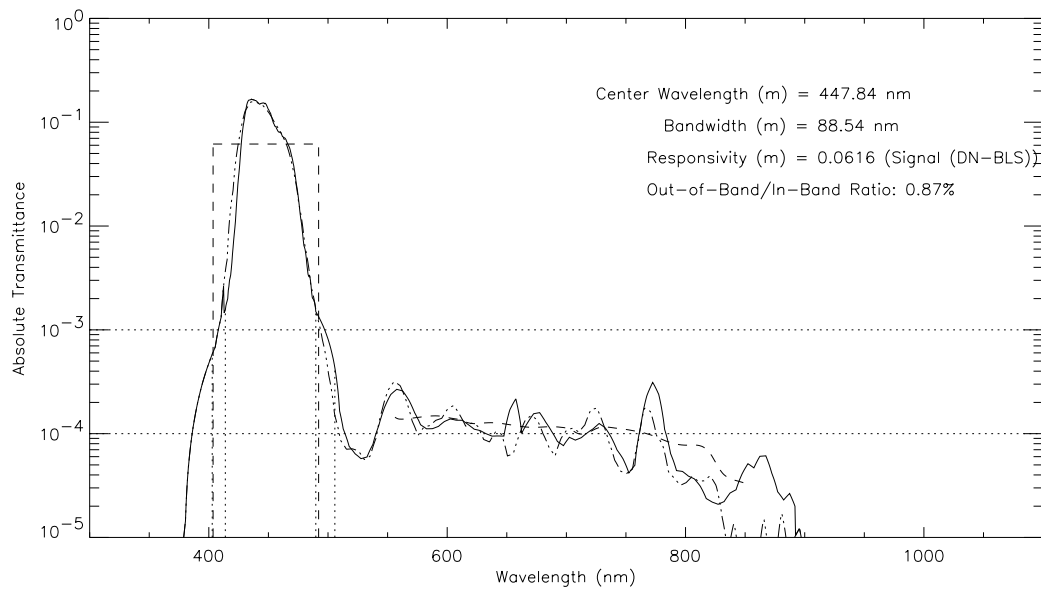


Figure 2. AirMISR measured spectral response profile for Band 1/ Blue.

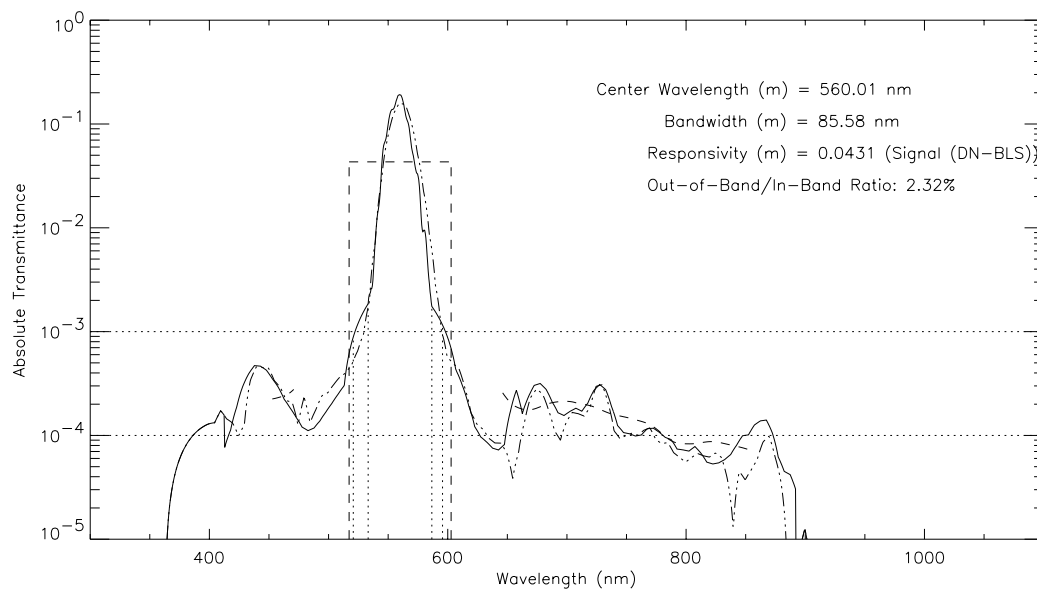


Figure 3. AirMISR measured spectral response profile for Band 2/ Green.

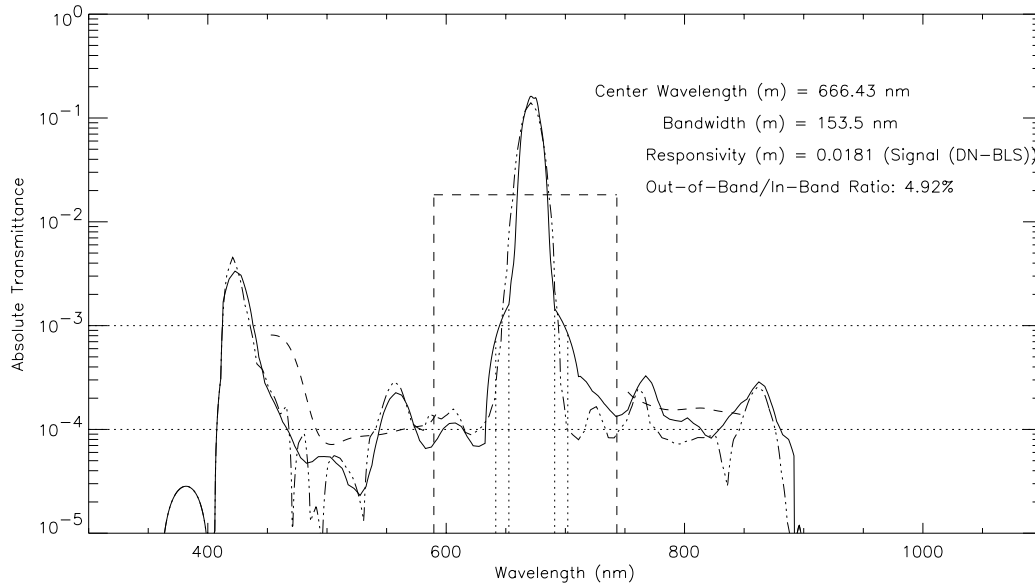


Figure 4. AirMISR measured spectral response profile for Band 3/ Red.

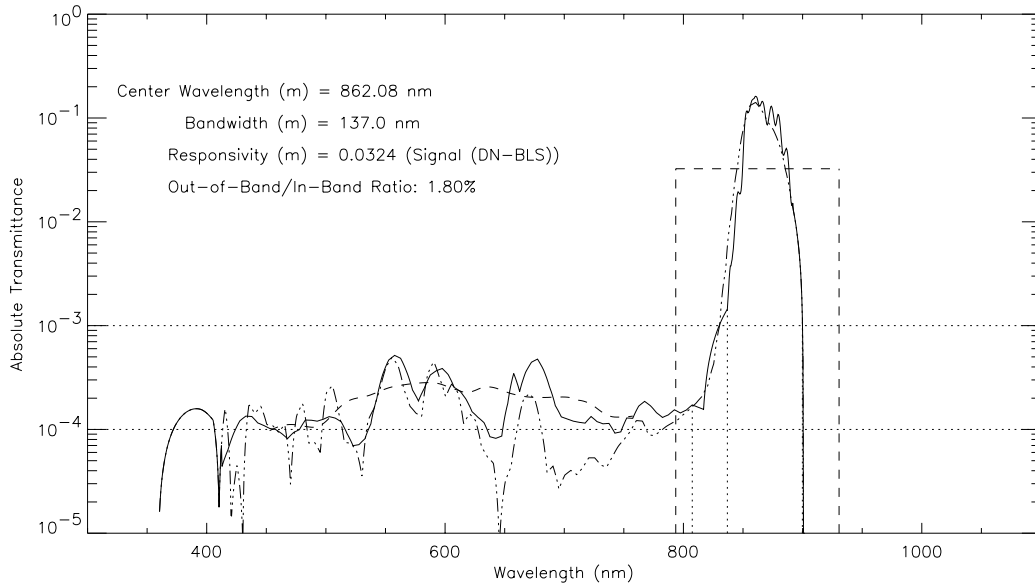


Figure 5. AirMISR measured spectral response profile for Band 4/ Near-infrared.

3. RADIOMETRIC CALIBRATION

The radiometric calibration of AirMISR is again accomplished by using heritage from the MISR program³. A 1.65 m (65") integrating sphere, with an exit aperture of 23 x 76 cm (9 x 30") is used for the flat-field source. This aperture, which fits over the 76 cm (30") circular sphere exit port, is used to minimize multiple reflections between the AirMISR or MISR cameras and the sphere exterior. Whereas MISR has been calibrated in a vacuum chamber, AirMISR has been calibrated at ambient pressure. This relaxation in the procedures is allowed in that the flight AirMISR focal plane temperature is approximately that of the

clean-room ambient temperature. No ambient-vacuum filter shifts occur with AirMISR (or MISR), as the focal planes are hermetically sealed.

The sphere output is placed on a radiometric scale by measurements made with detector standards. A QED-200 (made of United Detector Technology inversion layer diodes) is used to measure sphere output for the blue and green MISR spectral bands, Bands 1 and 2; and a QED-150 (made of Hamamatsu p-on-n photodiodes) is used for the red and near-infrared channels, Bands 3 and 4. Each detector is nearly 100% in internal quantum efficiency, for the wavelength regions at which they are operated, and is mounted in a light-trap configuration so as to collect the light reflected at each air/ detector interface. These standards are used with filters of the same spectral bandpass design as the flight cameras, and with a known field-of-view, established by use of a precision aperture tube. Traceability to Système International (SI) units is established through the measurement protocols of current, apertures, and aperture distances. JPL maintains working standards of voltage, resistance, and length which are traceable to the National Institute of Standards and Technology (NIST) or other international standards that are recognized by NIST.

The radiometric calibration is performed using the specific CCD integration times that are to be used during flight. These are determined such that the signal-to-noise ratio (SNR) specifications are just met at the edge-of-field, where the system transmittance is smallest. This allows the greatest margin between detector saturation and scene radiance. These integration times can be changed should the AirMISR sensor degrade. A recalibration of the focal plane would follow. The nominal integration times for the upcoming flight season have been determined to be 13.44, 18.88, 25.60, and 21.76 msec for Band 1/ Blue to Band 4/ NIR, respectively. A maximum integration time of 40.8 msec is allowable for each band.

The radiometric equation used to convert AirMISR output DN to band-averaged radiance is given by:

$$G_2(L^{\text{std}})^2 + G_1 L^{\text{std}} + G_0 = \text{DN} - \text{DN}_0 \quad (1)$$

where

- L^{std} is the incident radiance, weighted by S_λ , the band-specific standardized response profile [$\text{W m}^{-2} \text{sr}^{-1} \mu\text{m}^{-1}$],
- DN is the camera digital number,
- G_2 , G_1 , and G_0 are best fit parameters to the measured radiative transfer curve, and
- DN_0 is the digital number associated with the video offset voltage, unique for each line of data, and measured by the overclock pixels for that line.

The channel averaged coefficients for AirMISR are presented in Table 2.

Table 2. AirMISR array-averaged radiometric gain coefficients.

Spectral Band	G_0 , DN	G_1 , $\text{DN}/(\text{W m}^{-2} \text{sr}^{-1} \mu\text{m}^{-1})$	G_2 , $\text{DN}/(\text{W m}^{-2} \text{sr}^{-1} \mu\text{m}^{-1})^2$
Band 1/ Blue	9.88	23.26	4.34e-4
Band 2/ Green	21.17	23.82	1.15e-4
Band 3/ Red	51.77	28.92	1.89e-3
Band 4/ NIR	7.81	46.98	3.643e-3

There are several pixels within the AirMISR focal plane that are less responsive than their neighbors. These pixels can be identified by plotting the flat-field response of the camera, as shown in Figure 6. In particular there is a region in both Band 1/ Blue and Band 2/ Green of about 10 pixels in width, centered at pixel 1408, in which the response drop exceeds 10%. Further, for four pixels in this region the response drop exceeds 50%. For these pixels the signal-to-noise ratio (SNR) of the camera is

slightly smaller. For all pixels, however, the SNR specifications are met. Table 3 gives the array-averaged measured SNR as compared to the specification. The specification values listed here are interpolated from the illumination levels given in the original specifications document.

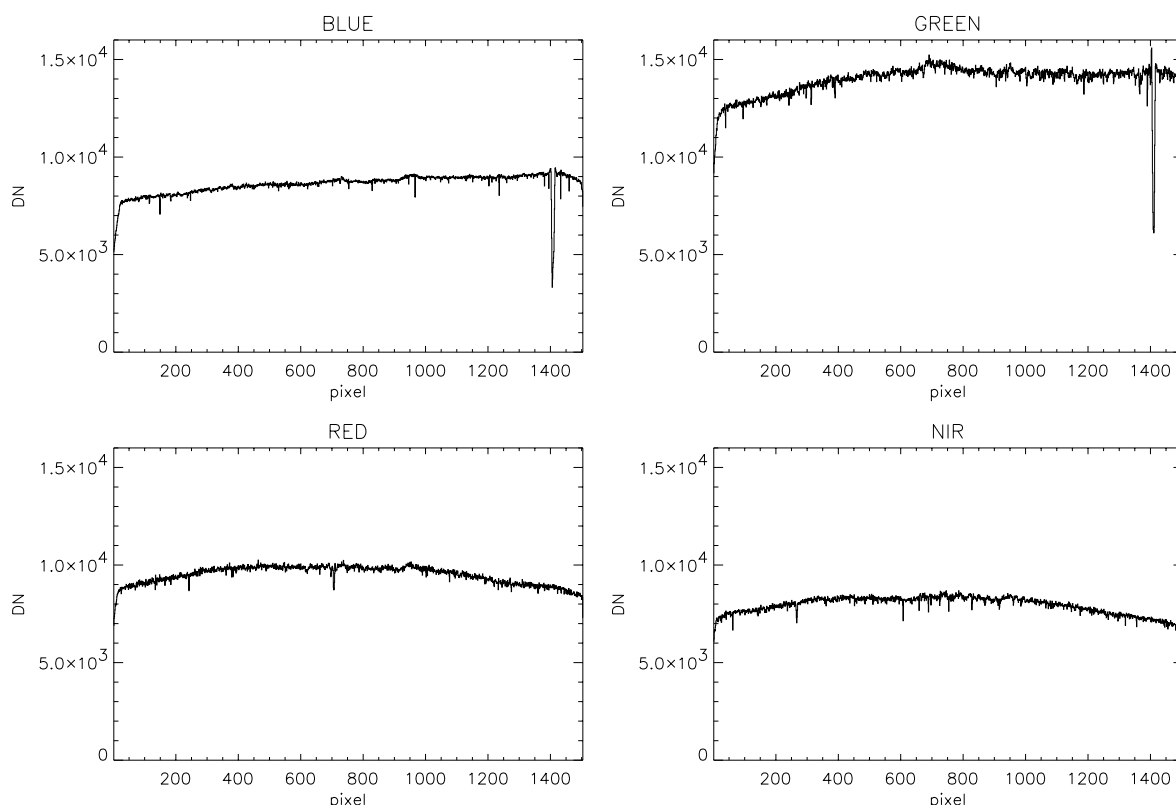


Figure 6. AirMISR response to a flat-field target.

Table 3. Band-averaged signal-to-noise ratios for AirMISR.

Spectral band	Test illumination: target equivalent reflectance level	SNR		
		Specification	Measured	Measured minimum
Band 1/ Blue	35.2%	103	759±74	376
Band 2/ Green	83.7%	148	969±91	646
Band 3/ Red	97.9%	114	775±74	693
Band 4/ NIR	104.8%	134	705±70	700

The radiometric uncertainties for this AirMISR laboratory calibration are the same as those reported for the MISR calibration⁴. All radiometric uncertainty specifications are believed to have been met for AirMISR. This includes a 3% absolute uncertainty (1σ) at an equivalent reflectance of 100% (that is near the upper end of the sensor response curve).

4. VICARIOUS CALIBRATION

MISR makes use of an on-board calibrator, as well as vicarious calibration experiments, in the determination of its in-flight radiometric response. The latter calibration is the process of ratioing a measure of the top-of-atmosphere radiance against the instrument output digital numbers, DN, obtained while imaging a uniform and bright earth target. One vicarious calibration approach to be explored for MISR is the utilization of an AirMISR underflight. The AirMISR data would facilitate the MISR calibration in two ways. First, agreement between AirMISR laboratory and vicarious calibrations will be used to verify the vicarious calibration input parameters used for MISR. That is, assuming a simultaneous AirMISR/ MISR overflight, the radiative transfer code inputs used to compute AirMISR 20 km radiances will likewise be used to generate MISR top-of-atmosphere radiances. As the AirMISR laboratory calibration can be done just prior to such an exercise, agreement between the laboratory and vicarious calibrations would allow us to assign a vicarious calibration to MISR with great confidence. Second, it is believed that AirMISR will be key in reducing the camera-camera relative uncertainty for MISR. AirMISR camera-camera relative calibrations, as determined in-flight, should be very precise, as it is only a single camera that is gimballed to the various view-angle positions. Simultaneous AirMISR/ MISR targeting will transfer this relative calibration to the MISR cameras.

A preliminary AirMISR vicarious calibration experiment was carried out on November 5, 1997. As this was an engineering flight for AirMISR, the experiment was not optimized for calibration exercises. The target was the tarmac outside the ER-2 hangers at Moffett Field, rather than the desired desert playas found in the southwest. Additionally, conditions were hazy, and surface characterization was made several days after the flight.

Instruments used in this study included the Analytical Spectral Devices Portable Field Spectrometer (ASD) radiometer, Portable Apparatus for Rapid Acquisition of Bidirectional Observation of the Land and Atmosphere (PARABOLA) III, and a Reagan sunphotometer. The ASD was used to provide spatial surface reflectance sampling of the area at a continuum of wavelengths. Using a Spectralon reflectance standard, the ASD data are used to derive the surface hemispherical-direct reflection factor (HDRF) for a nadir view angle. The surface HDRF is extended to the MISR view angles by using of the PARABOLA data. Atmospheric properties were determined by the Reagan sunphotometer. The aerosol, Rayleigh, and ozone components of optical depth were 0.025, 0.097, and 0.026, respectively, corresponding to a visibility of 23 km. With these, and a radiative transfer code (RTC), the band-weighted radiances are computed at 20 km. The RTC used by MISR is an adding-doubling code which accounts for multiple scattering. These radiance values are shown in Figure 7 by the asterisk symbols. These are compared to radiances derived from the instrument laboratory calibration. To do so, the image digital numbers of the tarmac target are radiance scaled using the laboratory gain coefficients. These radiances are shown by the solid line. Agreement is found to be quite good for these less than ideal conditions. Details of this experiment will be published elsewhere⁵.

5. ACKNOWLEDGMENTS

The design, calibration, and operation of AirMISR is attributed to a great number of individuals. David J. Diner is the Principal Investigator for MISR and AirMISR, and has defined the science performance requirements, data products, and experiment concept. Thomas G. Chrien and Charles G. Kurzweil were key players in the design of AirMISR. Jose Garcia, the AirMISR electrical engineer, was responsible for the acquisition of the laboratory calibration data presented here. He was assisted by Ghobad Saghri and Daniel Preston, MISR calibration engineers. James E. Conel is responsible for the AirMISR mission planning, and Mark C. Helmlinger acquired the in-situ measurements used to produce the vicarious calibration results. William C. Ledeboer has defined and produced the AirMISR radiometric products, and has assisted in evaluating AirMISR image data used for the vicarious calibration study. Stuart H. Pilorz is responsible for many of the algorithm development work utilized in the vicarious calibration experiments. The work described in this paper is being carried out by the Jet Propulsion Laboratory, California Institute of Technology, under contract with the National Aeronautics and Space Administration.

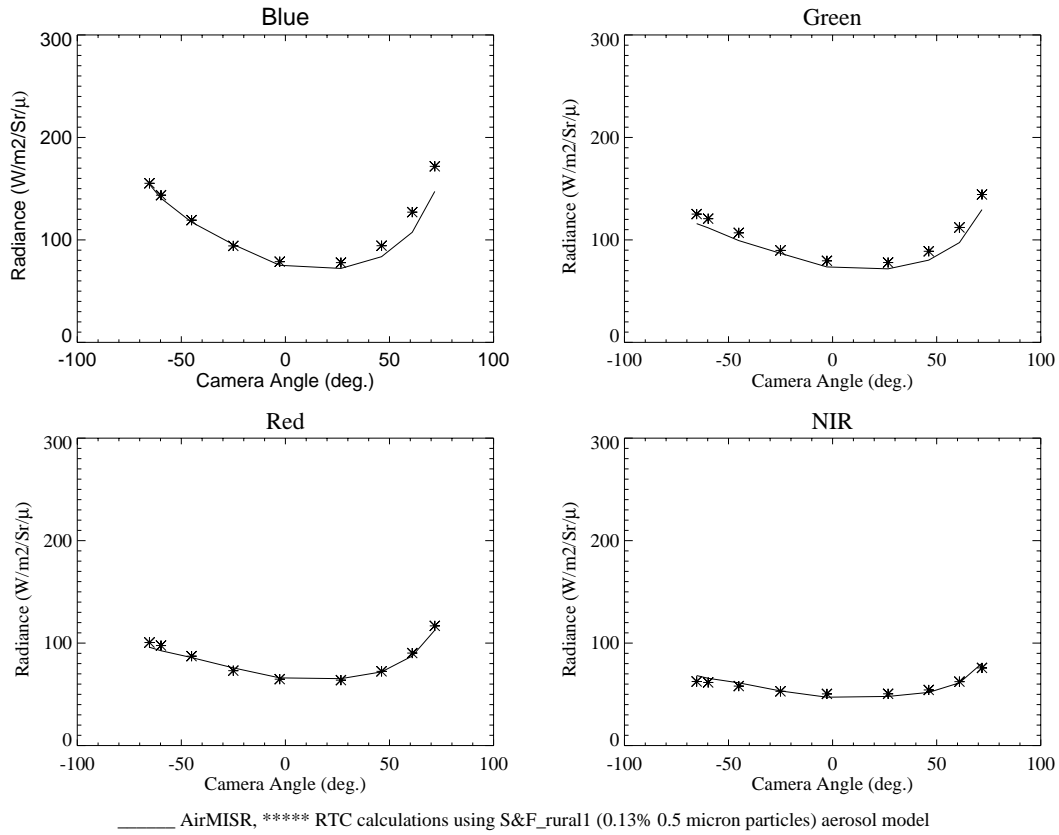


Figure 7. Comparison of AirMISR laboratory and vicarious calibrations.

6. REFERENCES

1. Diner, D.J., J.C. Beckert, T.H. Reilly, C.J. Bruegge, J.E. Conel, R. Kahn, J.V. Martonchik, T.P. Ackerman, R. Davies, S.A.W. Gerstl, H.R. Gordon, J-P. Muller, R. Myneni, R.J. Sellers, B. Pinty, and M.M. Verstraete (1998). Multiangle Imaging SpectroRadiometer (MISR) description and experiment overview. *IEEE Trans. Geosci. Rem. Sens.*, Vol. 36, 1072-1087.
2. Diner, D.J., L.M. Barge, C.J. Bruegge, T.G. Chrien, J.E. Conel, M.L. Eastwood, J.D. Garcia, M.A. Hernandez, C.G. Kurzweil, W.C. Ledeboer, N.D. Pignatano, C.M. Sarture, and B.G. Smith (1998). The Airborne Multi-angle SpectroRadiometer (AirMISR): instrument description and first results. *IEEE Trans. Geosci. Rem. Sens.*, Vol. 36, pp. 1339-1349.
3. Bruegge, C.J., V.G. Duval, N.L. Chrien, R.P. Korechoff, B.J. Gaitley, and E.B. Hochberg (1998). MISR prelaunch instrument calibration and characterization results. *IEEE Trans. Geosci. Rem. Sens.*, Vol. 36, pp. 1186-1198.
4. Bruegge, C.J., N. L. Chrien, R. A. Kahn, J. V. Martonchik, David Diner (1998). Radiometric Uncertainty Tabulations for the Retrieval of MISR Aerosol Products. Conference issue: New Developments and Applications in Optical Radiometry (NEWRAD '97), *Metrologia*. In press.
5. Abdou, W.A., C.J. Bruegge, M.C. Helmlinger, B.J. Gaitley, W.C. Ledeboer, S.H. Pilorz, J.E. Conel, and J.V. Martonchik (1998). Vicarious reflectance-based absolute radiometric calibration of AirMISR. *Remote Sens. of Environment*, in preparation.